International Journal of Pharmaceutics 434 (2012) 264–271

Contents lists available at SciVerse ScienceDirect

International Journal of Pharmaceutics

journal homepage: www.elsevier.com/locate/ijpharm

Enhanced solubility and oral bioavailability of itraconazole by combining membrane emulsification and spray drying technique

Young Keun Choi [a], Bijay K. Poudel [a], Nirmal Marasini [a], Kwan Yeol Yang [a], Jeong Whan Kim [a], Jong Oh Kim [a,***], Han-Gon Choi [b,**], Chul Soon Yong [a,*]

[a] College of Pharmacy, Yeungnam University, 214-1, Dae-Dong, Gyongsan 712-749, South Korea
[b] College of Pharmacy, Hanyang University, 55, Hanyangdaehak-ro, Sangnok-gu, Ansan 426-791, South Korea

ARTICLE INFO

Article history:
Received 15 April 2012
Received in revised form 5 May 2012
Accepted 19 May 2012
Available online 27 May 2012

Keywords:
Membrane emulsification
Spray-drying
Itraconazole
Solubility
Bioavailability

ABSTRACT

The objective of the present study was to enhance solubility and bioavailability of itraconazole by a combined use of membrane emulsification and spray drying solidification technique. A shirasu-porous-glass (SPG) membrane with a mean pore size of 2.5 μm was used to produce monodispersed microemulsions of itraconazole consisting of methylene chloride as the dispersed phase, a mixture of Transcutol HP and Span 20 as a stabilizer, and dextran as solid carrier dissolved in water as the continuous phase. The dispersed phase permeated through the SPG membrane into the continuous phase at an agitator speed of 150 rpm, a feed pressure of 15 kPa and a continuous phase temperature of 25 °C and the resultant emulsion was solidified using spray-drying technique. Solid state characterizations of the solid emulsion showed that the crystal state of itraconazole in solid emulsion was converted from crystalline to amorphous form. The solid emulsion of itraconazole displayed a significant increase in the dissolution rate than that of pure itraconazole. Furthermore, the solid emulsion after oral administration gave about eight-fold higher AUC and about ten-fold higher C_{max} in rats than pure itraconazole powder ($p < 0.05$), indicating this formulation greatly improved the oral bioavailability of drug in rats. Thus, these results demonstrated that the SPG membrane emulsification system combined with spray-drying technique could be used as a promising technique to develop solid formulation of itraconazole with enhanced solubility and bioavailability.

1. Introduction

Emulsions have been widely used in the industry of foods, cosmetics, and pharmaceuticals. They are conventionally prepared by using colloid mills, rotor–stator systems, ultra-sonic homogenizers and high-pressure homogenizers (McClements, 1999). Such methods employ extreme shear stresses of turbulence and high energy input to disrupt the dispersed phase or coarse emulsion to form submicrometer droplets. However, the droplets formed, though submicron, have broad size distribution and poor reproducibility, especially during scaling up and manufacturing. Pharmaceutical emulsions require precise degree of process controlling and optimization for the sake of dose proportionality which is difficult with conventional emulsification. Besides, these methods, owing to the application of high shear, are unsuitable for shear-sensitive ingredients like starches and proteins.

Many novel microporous emulsification techniques such as microengineered silicon nitride microsieves, ceramic α-aluminum oxide (α-Al_2O_3) membranes, polymeric membranes, shirasu porous glass (SPG) membrane have been developed to overcome these issues (Nakashima et al., 2000; Vladisavljević and Williams, 2005; Liu et al., 2011). Among them, SPG membrane has been reported to give highly controllable and uniform droplet size distribution (Nakashima et al., 2000). Developed by Nakashima and Shimizu (1993) and Nakashima et al. (1991) in the 1990s, SPG membrane emulsification produces emulsion by permeating a dispersed phase into an immiscible continuous phase through a SiO_2–Al_2O_3 glass membrane (commercially called SPG membrane) which has inter-connected cylindrical tortuous pore structures of fairly narrow pore diameters (0.1–20.0 μm). The dispersed phase is extruded through the membrane by applying relatively mild feed pressure built up with compressed N_2 and the droplets detach from the pores due to interfacial tension and the tangential shear exerted by flowing continuous phase along the membrane surface (Vladisavljević et al., 2007). The droplet size has linear correlation with pore size. This method is relatively simple and reliable and presents

* Corresponding author. Tel.: +82 53 810 2812; fax: +82 53 810 4654.
** Corresponding author. Tel.: +82 31 400 5802; fax: +82 53 400 5958.
*** Corresponding author. Tel.: +82 53 810 2813; fax: +82 53 810 4654.
E-mail addresses: jongohkim@yu.ac.kr (J.O. Kim), hangon@hanyang.ac.kr (H.-G. Choi), csyong@yu.ac.kr (C.S. Yong).

0378-5173/$ – see front matter © 2012 Elsevier B.V. All rights reserved.
http://dx.doi.org/10.1016/j.ijpharm.2012.05.039

many advantages over conventional methods like suitability to large scale production, controllable parameters, and reasonable energy consumption (Nakashima et al., 1991, 2000). Moreover, different process variables have been investigated in order to obtain small droplet sizes and highly monodispersed microspheres, nano/microemulsions, and multiple emulsions (Omi et al., 1997; Vladisavljević and Schubert, 2003; Vladisavljević et al., 2006; Nazir et al., 2011; Oh et al., 2011).

Dry emulsion represents a potential oral drug delivery system for BCS class II drugs which have low aqueous solubility and consequently low bioavailability and high intra- and inter-subject variability. Dry emulsion overcomes the limitation of liquid emulsions such as lack of physicochemical instability (coalescence, creaming, phase inversion, and so on) and patient compliance problems. Solid state emulsion, referring to the dispersion of an immiscible oil phase within a solid-phase, can be obtained by removal of the aqueous phase of liquid emulsion by spray-drying (Yan et al., 2011), lyophilization (Chen et al., 2011) and solvent evaporation (Myers and Shively, 1993; Shively and Thompson, 1995).

Thus, in the present study, the optimized liquid emulsion containing itraconazole, a broad-spectrum triazole antimycotic drug (Saag and Dismukes, 1988; Odds et al., 2000) was prepared using membrane emulsification technique, first by controlling the process parameters affecting droplet size and size distribution such as continuous phase temperature, agitator speed, and feed pressure. Then, the resulted liquid emulsion was further developed into solid form using spray drying process, and the physicochemical properties of solid emulsion were investigated using SEM, DSC, and X-ray diffraction. The in vitro dissolution and pharmacokinetic profiles of solid emulsion in rats was further evaluated compared to itraconazole powder.

2. Materials and methods

2.1. Materials

Itraconazole was supplied from Dongwha Pharm. Co., Ltd. (Anyang, South Korea). Polyglycolyzed glycerides (Labrafil M 1944CS, Labrafil M 2125CS, Capryol 90, Lauraglycol FCC, Labrafac, Labrasol, Transcutol HP) were kind-heartedly donated by Gattefosse Co. (St. Priest, France). Castor oil was supplied by Sigma (St. Louis, USA). Span 20, Span 80, Tween 20, Tween 80, methylene chloride, and dextran were purchased from DC chemical Co. (Seoul, South Korea). A miniature kit for emulsification with an MPG module (microporous glass, a brand name of SPG) was purchased from Kiyomoto Iron Works Co. (Miyazaki, Japan). Distilled water was prepared freshly whenever required. All other chemicals were of reagent grade and used without further purification.

2.2. Solubility study

An excess amount of itraconazole (approximately 100 mg) was placed in a 2 ml micro tube (Axygen MCT-200) containing 1 ml of various vehicles. Then, the mixture was vortexed and shaken for 3 days at 25 °C in a shaking water-bath (100 St/min) for equilibrium. The samples were centrifuged at 3000 × *g* for 15 min (Eppendorf, USA) and filtered through a membrane filter (0.45 μm) to remove the undissolved itraconazole (Balakrishnan et al., 2009; Choi et al., 1998; Li et al., 2008). The supernatant was taken and diluted with ethanol for quantification of itraconazole by HPLC system (Hitachi, Tokyo, Japan) consisting of Ez chrom elite (version 318a) computer software, Hitachi L-2130 pump and Hitachi L-2400 UV-VIS detector. Column was Inertsil ODS-3 reverse-phase C18 column, 5 μm, 15 cm × 4.6 mm). Mobile phase consisted of acetonitrile and 0.05% diethylamine in distilled water (70:30, v/v), adjusted to pH 6.0 with 30% acetic acid. Mobile phase was filtered through 0.45 μm membrane filter and eluted at a flow rate of 1.2 ml/min. The effluent was monitored at a UV absorption wavelength of 254 nm.

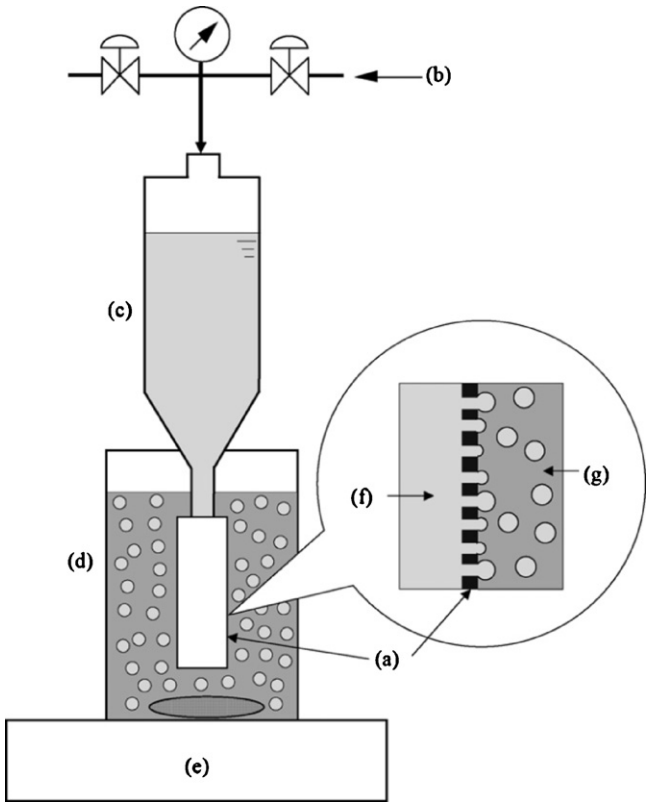

Fig. 1. Schematic diagram of the experimental apparatus used for the preparation of O/W emulsions using an SPG membrane: (a) SPG membrane module; (b) compressed nitrogen gas; (c) dispersed phase container; (d) continuous phase and emulsion container; (e) magnetic stirrer and heater; (f) dispersed phase; (g) continuous phase.

2.3. Construction of pseudo-ternary phase diagram

The pseudo-ternary diagrams were constructed by titration of homogeneous mixture of surfactant (mixture of Transcutol HP and Span 20 at 1:1, w/w ratio) and water with the organic phase. Briefly, surfactant and water were weighed at different ratios (0:1 to 1:3, v/v) in the vials, and were vortexed vigorously for 1 min. Then, the organic phase (methylene chloride) was slowly added in 5% increments to each mixture, vortexed for 5 min and equilibrated in a water bath at 25 °C for 1 h. These samples were visually assessed for phase clarity (Shafiq et al., 2007). Clear and isotropic samples were judged to be within the microemulsion domain (Craig et al., 1995) and no attempts were made to identify the other regions of the phase diagrams.

2.4. Experimental set-up and procedure

A miniature kit for emulsification with a MGP module (microporous glass, a brand name of SPG) was purchased from Kiyomoto Iron Works Co. (Miyazaki, Japan). A schematic diagram of a typical small-scale, membrane emulsification apparatus, representative of those in the literature for making o/w emulsions, is shown in Fig. 1. The system incorporates a tubular microfilteration membrane, a pump, a feed vessel, and a pressurized (N_2) oil container. The hydrophilic SPG membrane was tube-shaped with an outer diameter of 10 mm, a thickness of 0.75 mm and a pore size of 2.5 μm. 5 g of

methylene chloride containing 2 g of itraconazole (dispersed phase) were stored in a pressure-tight vessel that was connected to a nitrogen gas inlet attached to a pressure gauge PG-200-163GP-S (COPAL electronics, Tokyo, Japan). The continuous phase, 100 g of water containing 5 g surfactant mixture and 2.5 g dextran, was stirred gently with magnetic stirrer bar (3 cm long) in a beaker to prevent the creaming of the droplets. The dispersed phase is pumped under N_2 gas pressure through the pores of the membrane into the aqueous continuous phase which circulates through the middle of the membrane. The experiments were carried out over a wide range of agitator speeds (150–700 rpm), feed pressures (15–40 kPa), and continuous phase temperatures (25–35 °C).

2.5. Determination of mean droplet size, droplet size distribution

The droplet size (*z*-average particle diameter) and polydispersity index (PDI) of all samples were measured using a NanoZS light scattering particle size analyzer (Malvern Instruments, Malvern, UK) at a wavelength of 635 nm and scattering angle of 90°. All the experiments in the study were performed in triplicates at 25 ± 0.1 °C and the data were expressed as the mean ± standard deviation (S.D.). A two-tailed unpaired Student's *t*-test was performed at $p < 0.05$.

2.6. Preparation of solid emulsion

Solid emulsion of itraconazole was prepared by a Büchi 190 nozzle type mini spray dryer (Flawil, Switzerland). The liquid emulsion pre-warmed to 60 °C was delivered to the nozzle (0.7 mm diameter) at a flow rate of 5 ml/min using a peristaltic pump and spray-dried at 130 °C inlet temperature and 75–80 °C outlet temperature. The aspirator was set at 85%, the pump at 10%, and the air flow was 600 l/h. The direction of air flow was the same as that of sprayed products (Choi et al., 2001; Li et al., 2008).

2.7. Characterization of the solid emulsion

2.7.1. Morphological analysis of solid emulsion

Scanning Electron Microscopy (SEM) photomicrographs were taken to compare the crystal morphology of itraconazole powder, dextran, physical mixture, and the solid emulsion. The outer macroscopic structures were investigated by S-4100 scanning electron microscope (Hitachi, Tokyo, Japan). The samples were fixed on a brass-stub using double-sided adhesive tape and made electrically conductive by coating in a vacuum (6 Pa) with platinum (6 nm/min) using Hitachi Ion Sputter (E-1030) for 240 s at 15 mA. The SEM images were analyzed with an image analysis system (ImageInside Ver 2.32).

2.7.2. Differential scanning calorimetry (DSC)

The thermal analysis of itraconazole powder, dextran, physical mixture, and itraconazole loaded-solid emulsion was carried out using a differential scanning calorimetry (DSC Q200 v24.2 build 107, TA Instruments, New Castle, DE, USA). The samples (about 1.50 mg) were placed in standard aluminum pans, and dry nitrogen was used as effluent gas. All samples were scanned at a temperature ramp speed of 10 °C/min and the heat flow from 70 to 180 °C.

2.7.3. Powder X-ray diffraction (P-XRD)

The P-XRD patterns of itraconazole powder, dextran, physical mixture, and itraconazole loaded solid emulsion were measured by the X'Pert PRO diffractometer (PAN analytical, Netherlands) at room temperature using monochromatic Cu Kα-radiation (λ = 1.5406 Å) at 30 mA and 40 kV over a range of 2θ angles from 10° to 50° with an angular increment of 0.02°/s (Li et al., 2008).

2.8. Dissolution study

Dissolution profiles of itraconazole powder and itraconazole-loaded solid emulsion were determined in water. The accurately weighed samples equivalent to 100 mg of itraconazole were filled in size 0 gelatin capsules. The dissolution test was performed at 36.5 °C using the basket method at 100 rpm with 900 ml water as the dissolution medium. 5 ml of dissolution samples were collected at 5, 10, 15, 30, 45, 60, 90, and 120 min and immediately followed by addition of an equal volume of fresh dissolution media maintained at the same temperature to keep the volume of dissolution media constant and to maintain the sink condition (Choi et al., 1998; Yong et al., 2005). The withdrawn samples were filtered through a membrane filter (0.45 μm) and analyzed using the HPLC.

2.9. Pharmacokinetic study

All surgical and experimental procedures involving animals were in accordance with the Guiding Principles in the Use of Animals in Toxicology, as adopted by the Society of Toxicology (SOT, 2008). The procedures were also reviewed and approved by the Institute of Laboratory Animal Resources of Yeungnam University.

2.9.1. In vivo experiment

Male Sprague-Dawley rats weighing 290 ± 20 g were fasted for 12 h prior to the experiments but allowed free access to water. Twelve SD rats were divided into two groups. The femoral artery of each rat, anaesthetized in an ether-saturated chamber, was cannulated with polyethylene cannula (PE-50). The cannula was flushed with 0.3 ml of heparinized normal saline solution (80 IU) to prevent blood clotting. After rats recovered from the anesthesia, itraconazole powder and solid emulsion (equivalent to 15 mg/kg dose of itraconazole) were administered orally to rats using oral sonde. Each preparation was dispersed into 500 μl of distilled water by vortexing for about 20 s immediately prior to dosing. After dosing the rats, 300 μl of the blood was collected at designated time interval. The blood samples were centrifuged at 3000 × *g* for 10 min and the plasma was immediately stored at −20 °C until further analysis.

2.9.2. Plasma drug concentration analysis

The concentration of itraconazole in rat plasma was determined by HPLC as follows: 50 μl of fenofibrate solution as an internal standard (2 μg/ml in acetonitrile) was added into 200 μl of plasma. The mobile phase consisted of a mixture of acetonitrile:water (60:40, v/v). Mobile phase was filtered under vacuum and degassed before use. For the extraction, 1.5 ml of t-butyl methyl ether was added and the mixture was vortex-mixed for 2 min. After centrifugation (10 min, 10,000 × *g*) the organic layer was collected and evaporated to dryness under vacuum (Modul 3180C, BioTron Co., Puchon, South Korea) at 40 °C. The residue was dissolved in 100 μl of mobile phase and 30 μl was injected into the HPLC system described in Section 2.2. The standard curve showed excellent linearity in the concentration range of 10–2000 ng/ml of itraconazole. Relative standard deviation (RSD) at different concentrations and time was less than 5%. The lowest standard on the plasma calibration curve with 10 ng/ml concentration was considered as the lower limit of quantification (LOQ) with identifiable and reproducible peak.

3. Results and discussion

3.1. Solubility study

The choice of a suitable surfactant is important for the production of uniformly sized emulsion droplets via SPG membrane emulsification. Cationic surfactants were reported to be electrostatically attracted to the anionic silanol groups on the membrane

Table 1
Solubility of itraconazole in various surfactants.

Surfactants	Solubility (mg/ml)[a]
Tween 20	0.98 ± 0.07
Tween 80	0.91 ± 0.14
Span 20	1.06 ± 0.52
Span 80	0.43 ± 0.03
Labrafil M 1944 CS	0.27 ± 0.01
Labrafil M 2125 CS	0.14 ± 0.12
Capryol 90	1.22 ± 0.08
Lauraglycol FCC	0.42 ± 0.04
Labrasol	1.45 ± 0.09
Transcutol HP	3.08 ± 0.11
Labrafac	0.18 ± 0.00

[a] Each value represents the mean ± S.D. ($n = 3$).

surface (Schröder and Schubert, 1999) and were hence avoided in the solubility screening. Though anionic surfactants like sodium dodecyl sulfate (SDS) were reported to give emulsions with smaller droplets and smaller PDI in SPG emulsification (Schröder et al., 1998), only non-ionic surfactants with high hydrophilic–lipophilic balance (HLB) were screened because of safety concerns. The solubilities of itraconazole in the various vehicles were investigated, as shown in Table 1. Among the surfactants tested in this study, Transcutol HP (3.08 ± 0.11 mg/ml) and Span 20 (1.06 ± 0.52 mg/ml) were selected as the surfactant and co-surfactant based on their solubility for itraconazole and preliminary studies. Transcutol HP is a powerful solubilizing agent used in several dosage forms on account of its ability to solubilize many drugs (Torrado et al., 1997; Kim and Park, 2004). The addition of Span 20 as co-surfactant has been shown to increase the extent of the microemulsion region in SMEDDS formulations. From these results, we selected Transcutol HP and Span 20 as surfactants, and methylene chloride was used as the oil phase.

3.2. Pseudo-ternary phase diagrams

Phase diagrams were constructed to determine the proportion of components that can result in maximum microemulsion existence. As shown in Fig. 2, a larger emulsion region was obtained in the system in which the surfactant mixture was used. The mixture of Transcutol HP/Span 20 (1:1) was selected as the surfactant. Furthermore, based on the preliminary experiments on particle size and size distribution (data not shown), the formulation composed of methylene chloride, water, and the surfactant mixture at the weight ratio of 5/100/5 was selected as the basic component for further studies.

3.3. Influence of process parameters on mean droplet size and distribution

3.3.1. Effect of continuous phase temperature on droplet size

Temperature of the continuous phase is one of the important parameters in emulsification affecting both the viscosity of the dispersed and continuous phases and also the nature of the emulsifier as a consequence of the phase inversion temperature and its solubility (Joscelyne and Trägårdh, 1999). The alteration in interfacial tension between the oil and the water phase at higher temperatures could lead to coarsening of the emulsion via Ostwald ripening and/or coalescence (Tadros et al., 2004; Ee et al., 2008). In addition, there might be the fluctuation in interfacial tension because of the increased temperature that might lead to the low uniformity of the emulsion droplets (Babak et al., 2007; Soheil et al., 2008). It has been reported that temperature influences the uniformity of emulsions during microporous membrane emulsification (Oh et al., 2011). In this study, methylene chloride used as the oil phase, has a very low evaporation temperature of 40 °C. The interfacial tension

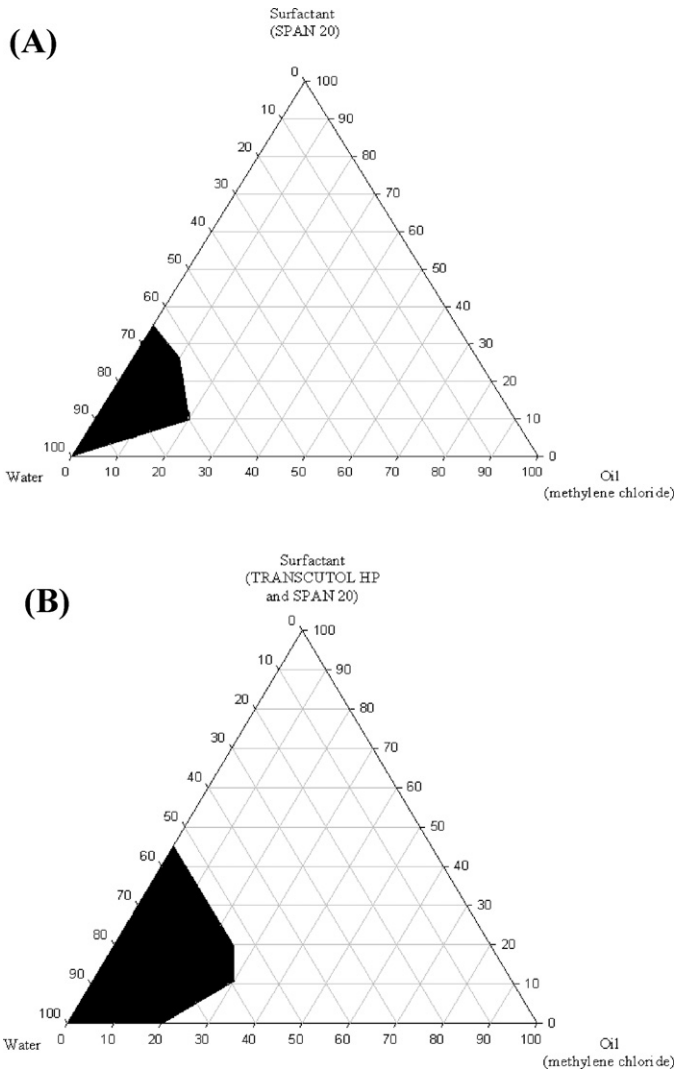

Fig. 2. Pseudo-ternary phase diagram of formulation: (A) Span 20, methylene chloride, and water; (B) Span 20:Transcutol HP, methylene chloride, and water. Black regions show the domain of efficient emulsification.

between the two phases would change at a higher temperature. Therefore, the *z*-average particle size and size distribution of emulsion droplets formed by the SPG membrane emulsification method were investigated as a function of temperature ranging from 25 °C to 35 °C. As demonstrated in Fig. 3A, preparation of emulsions at a continuous phase temperature of 25 °C resulted in the smallest mean droplet size with a narrow size distribution. However, as the continuous phase temperature was increased from 25 to 35 °C, the mean droplet size increased from ca. 410 nm to ca. 450 nm, accordingly, and the polydispersity index increased from 0.153 ± 0.014 to 0.333 ± 0.034, which indicated that the monodispersity of the microemulsions gradually became worse with the increase in temperature. Thus, 25 °C was selected as the optimal continuous phase temperature for preparation of the microemulsion because it gave relatively uniform emulsion droplets with a narrow particle size distribution.

3.3.2. Effect of agitating speed on droplet size

The influence of agitator speed over a range of 150–700 rpm on the *z*-average diameter of emulsion droplets is shown in Fig. 3B. The *z*-average diameter and PDI increased sharply as the agitator speed increased to 700 rpm. Indeed, various postulations have been made regarding the speed of the agitator in order to explain the

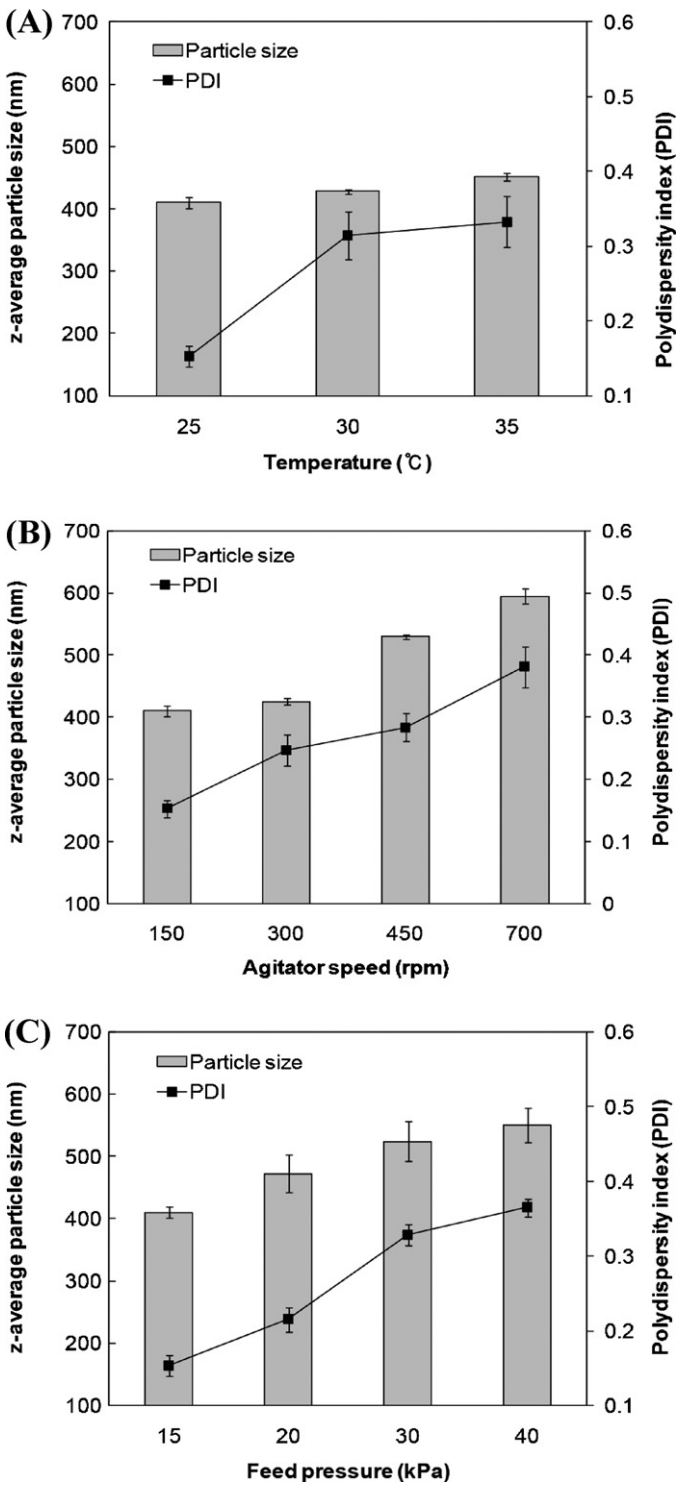

Fig. 3. Effect of: (A) continuous phase temperature, (B) agitating speed, and (C) feed pressure of the dispersion phase on the *z*-average diameter and size distribution of the emulsion droplet. Each value represents the mean ± S.D. ($n = 3$).

mechanism of emulsion formation (Ni et al., 2007; Wei et al., 2009). However, the effects of agitator speed on the properties of an emulsion have not yet been clarified. In one previous study, for instance, it was reported that the particle size of emulsions decreased as the agitator speed increased (Tsukada et al., 2009), while another study reported that the particle size increased sharply as the agitator speed increased to a certain rpm and then showed no significant change in particle size upon further increases (Oh et al., 2011). The magnitude of shear on the droplets forming on the membrane surface is proportional to the agitating speed. In higher agitating speeds, the increased shear and the fluid mechanical stresses might have increased the chance of collisions between droplets while forming, thereby causing the coalescence of droplets and increasing the droplet size. It has been reported that the spontaneous droplet detachment from the membrane at low flow rate of continuous phase and low feed pressure favored the production of more uniform emulsion than the droplet detachment driven by wall shear stress due to moving continuous phase (Yasuno et al., 2002; Kobayashi et al., 2003). An increase in the agitation speed might give rise to an associated increase in energy consumption. Thus, as the agitation speed increased, the particle size distribution in the emulsion became broader. Our results suggest that an agitator speed of 150 rpm is the optimal speed, since it produced emulsion droplets with a relatively smaller *z*-average diameter with narrow size distribution under this set of conditions.

3.3.3. *Effect of feed pressure on dispersion phase*

Feed pressure is known to be another key factor that influences the formation of an emulsion and particle size distribution. By controlling feed pressure in the emulsification process, the flux rate of the dispersed phase across the membrane channel, as well as the detachment of the droplets, can be modulated for the preparation of uniform emulsion droplets. Higher feed pressures are required for membranes of smaller nominal pore size, given that all other parameters are the same, because of the higher capillary pressures. Increasing feed pressure increases the flux of dispersed phase through a membrane in accordance with Darcy's law (Schröder et al., 1998). Too high pressures lead to jets of oil and very large droplets, whereas low flux of the dispersed phase by low pressures resulted in a long emulsification time, which is unsuitable for volatile dispersed phase like methylene chloride. Long emulsification time may lead to the escaping of volatile dispersed phase, thus changing the optimum proportion of the formulation. Fig. 3C shows that an increase in feed pressure of the dispersion phase from 15 kPa to 40 kPa resulted in a gradual increase in the diameter of *z*-average emulsion droplets from ca. 410 to ca. 550 nm. Such increase in the mean droplet size was due to the droplet growth and coalescence at the membrane surface within the period of decreasing interfacial tension. Similar results were also observed in previous studies (Schröder et al., 1998; Schröder and Schubert, 1999; Vladisavljević and Schubert, 2003). In addition, increase of feed pressure caused the polydispersity index to increase, which may be either due to the collision of the dispersed phase particles with the continuous phase components thereby breaking the emulsion or the delicate force balance against the interfacial tension was broken, thereby resulting in a non-uniform size distribution of the emulsion droplets. However, lower feed pressures below 15 kPa, was not enough to permeate the dispersed phase out of the membrane. Thus, feed pressure of 15 kPa was used as an optimal condition for the preparation of liquid emulsion in further studies.

Based on these findings, the formulation composed of itraconazole, oil, water, surfactant mixture, and dextran at the weight proportion of 2/5/100/5/2.5 was selected to produce an optimal uniform emulsion using an SPG membrane at an agitator speed of 150 rpm, a feed pressure of 15 kPa and a continuous phase temperature of 25 °C.

3.4. *Solid state characterization of solid emulsion*

The solid emulsion was prepared by spray-drying of aqueous solution containing liquid emulsion and dextran as a hydrophilic solid carrier. The *z*-average diameters of the liquid emulsion and the reconstituted solid emulsion were 410.4 ± 8.9 nm and 452.6 ± 18.6 nm, respectively. The polydispersity index (PDI) of

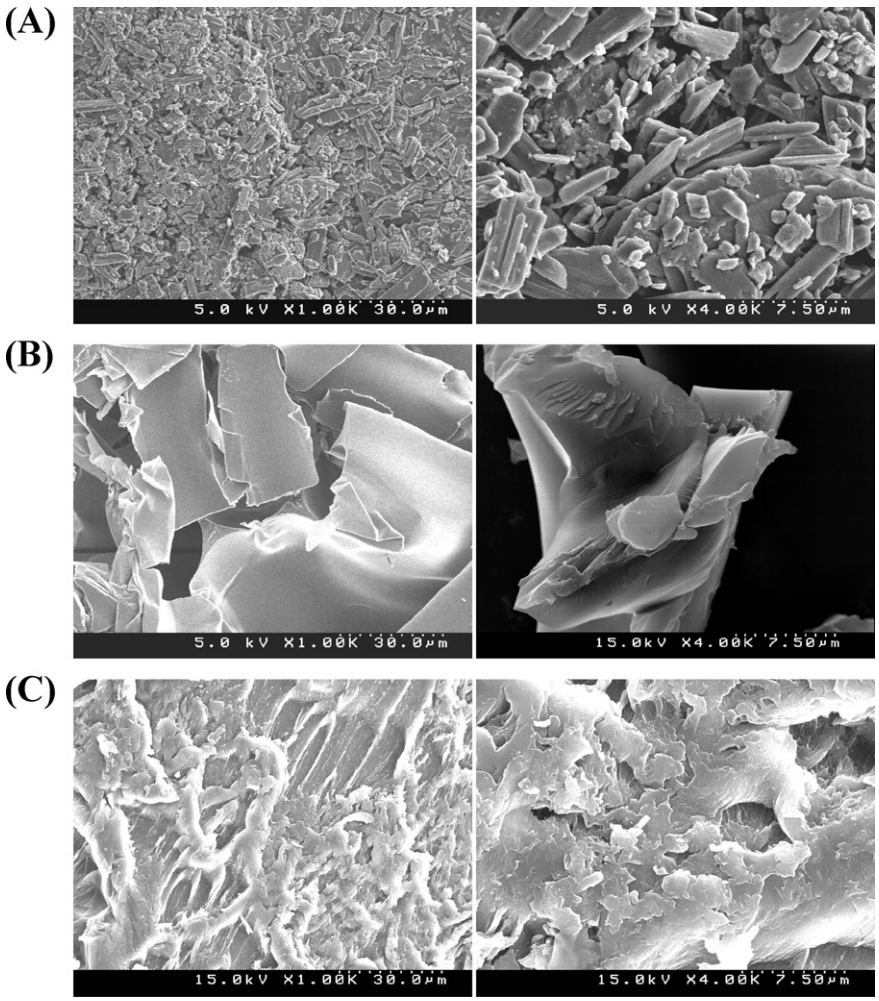

Fig. 4. Scanning electron micrographics of: (A) itraconazole (1000× and 4000×), (B) dextran (1000× and 4000×), and (C) solid emulsion (1000× and 4000×).

liquid emulsion and solid emulsion prepared with dextran were 0.153 ± 0.014 and 0.245 ± 0.04, respectively. Dextran, a hydrophilic carrier, produced the solid emulsion with slightly larger emulsion droplet size compared liquid emulsion. However, like the liquid emulsion, this solid emulsion produced micro-sized emulsion droplet.

The structural characteristics of itraconazole powder, dextran, and solid emulsion are clearly visible in their SEM images, as shown in Fig. 4. The SEM images of itraconazole powder revealed solid cubes (Fig. 4A), which was similar to previous reports (Al-Marzouqi et al., 2006). On the other hand, dextran appeared as smooth-surfaced and connected structure (Fig. 4B). The morphology of solid emulsion, formulated with itraconazole, surfactants, and dextran gave relatively rough surface, suggesting that drug might be attached and dispersed onto the surface of the solid carrier, dextran (Fig. 4C). Such molecular dispersion of the drug on the solid carrier may account for the enhanced drug release and absorption.

The DSC thermographs of itraconazole, dextran, physical mixture, and solid emulsion are shown in Fig. 5A. The crude itraconazole was characterized by a single, sharp melting endothermic peak at 171 °C, in agreement with its melting point and crystalline nature. Dextran gave no intrinsic peaks found in the DSC curves between 70 °C and 180 °C. In the physical mixture of drug and excipients, a melting peak of 171 °C was observed with a reduced intensity due to the dilution effect, indicating that the drug was still in crystalline form. However, no characteristic endothermic peak of drug was found in the DSC curves of the solid emulsion, indicating that itraconazole was highly dispersed in solid emulsion as a molecular or amorphous state.

The powder XRD patterns of itraconazole, dextran, physical mixture, and solid emulsion are presented in Fig. 5B. As expected, the raw itraconazole had sharp peaks at diffraction angles due to its typical crystalline structure, while dextran showed no intrinsic peaks in the XRD. In the physical mixture of drug and excipients, all the major characteristic crystalline peaks of drug were observed. However, the solid emulsion showed had no characteristic peaks, showing the absence of drug crystals. Thus, itraconazole was present in a changed amorphous state in the solid emulsion prepared with dextran, which is in good agreement with DSC results.

3.5. Dissolution study

Fig. 6 illustrates the dissolution of itraconazole from drug powder and solid emulsion in water. As expected, the drug powder displayed low dissolution rate due to its low aqueous solubility. On the other hand, dissolution rate from the solid emulsion was found to be significantly higher as compared with that of crude itraconazole powder. Notably, the drug from solid emulsion was released rapidly and reached about 80% within 10 min. It could be suggested that the solid emulsion resulted in spontaneous formation of a microemulsion with a small droplet size (Yan et al., 2011),

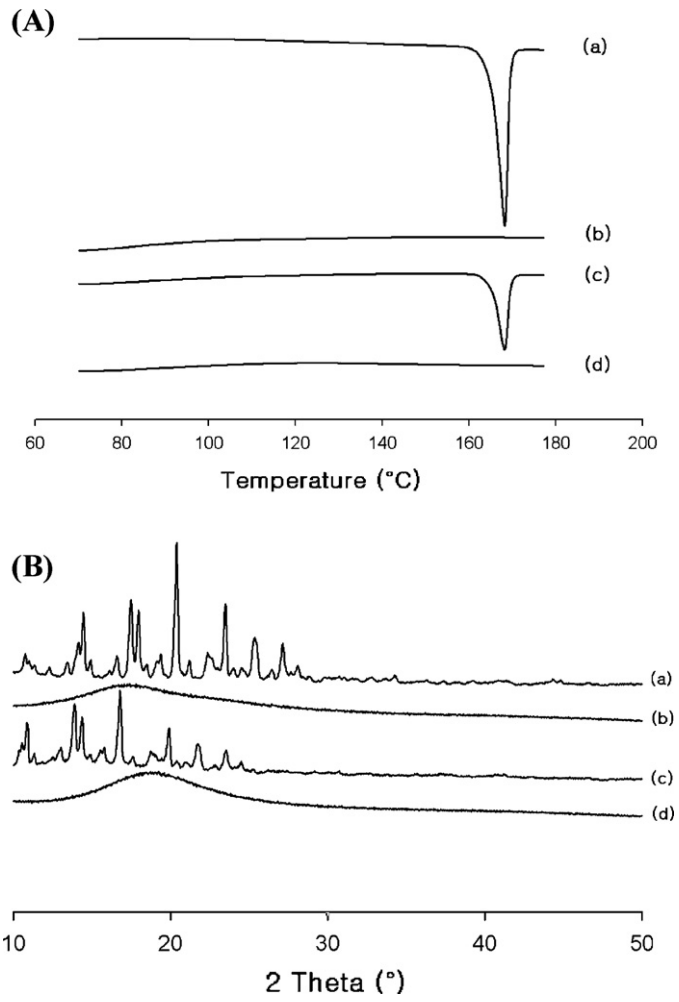

Fig. 5. (A) Differential scanning calorimetric thermograms and (B) Powder X-ray diffraction. (a) Itraconazole powder, (b) dextran, (c) physical mixture, and (d) solid emulsion.

which permitted a much faster dissolution rate than that of itraconazole powder. Thus, these results suggested rapid and complete release dissolved itraconazole from solid emulsion could lead to higher absorption and higher oral bioavailability.

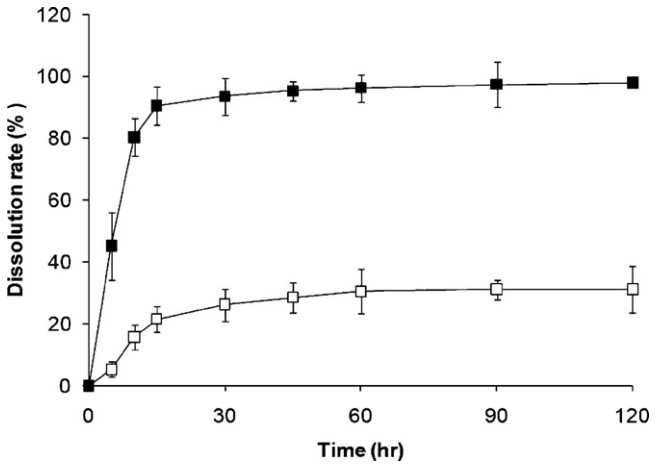

Fig. 6. Dissolution profiles of the drug from the itraconazole powder (□) and solid emulsion (■). Each value represents the mean ± S.D. (n = 6).

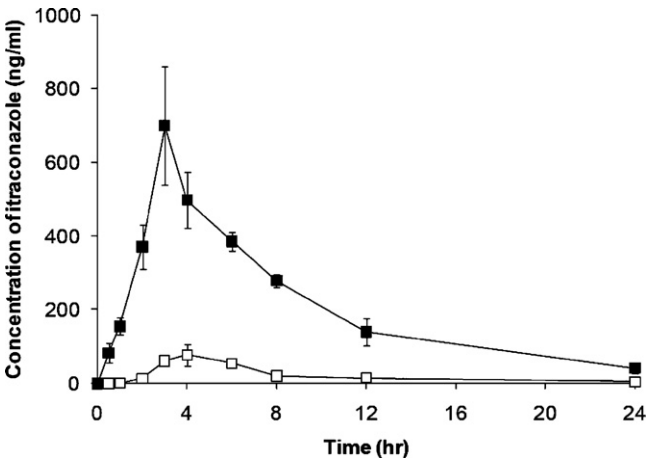

Fig. 7. Plasma concentration-time profiles of drug after oral administration of itraconazole powder (□) and solid emulsion (■) at the dose of 10 mg/kg as itraconazole to rats. Each value represents the mean ± S.D. (n = 6).

Table 2
Pharmacokinetic parameters of itraconazole after oral administration of itraconazole powder and solid emulsion to rats.

Parameters	Itraconazole powder	Solid emulsion
AUC (ng h/ml)	583.20 ± 103.37	4833.94 ± 1534.80*
C_{max} (ng/ml)	48.22 ± 11.67	494.66 ± 60.17*
T_{max} (h)	4.45 ± 0.51	3.60 ± 0.69
K_{el} (h^{-1})	0.23 ± 0.01	0.28 ± 0.03

Each value represents the mean ± S.D. (n = 6).
* $p < 0.05$, compared with the powder.

3.6. Pharmacokinetic study

Fig. 7 shows the change of mean plasma concentration of itraconazole after oral administration of preparations at a dose of 15 mg/kg itraconazole in rats. The total plasma concentrations of drug in solid emulsion were significantly higher compared with those in itraconazole powder. In particular, the initial plasma concentrations of itraconazole from solid emulsion were significantly higher than those from itraconazole powder ($p < 0.05$). The corresponding pharmacokinetic parameters of itraconazole are listed in Table 2. At the same dose of 15 mg/kg, the solid emulsion gave significantly higher AUC and C_{max} of itraconazole than did itraconazole powder ($p < 0.05$). AUC value of the solid emulsion increased around 8-fold than that of powder, indicating this formulation greatly improved the oral bioavailability of drug. However, the T_{max} value of solid emulsion was faster than that of itraconazole powder but not significant. In vivo studies demonstrated that the enhanced oral bioavailability of itraconazole from solid emulsion might have contributed to the marked increase in the absorption rate of itraconazole due to the faster dissolution of itraconazole from the solid emulsion in the initial phase.

4. Conclusion

An emulsion system composed of itraconazole, oil, water, surfactant mixture, and dextran at the weight ratio of 2/5/100/5/2.5 was prepared using an SPG membrane emulsification technique at an agitator speed of 150 rpm, a feed pressure of 15 kPa and a continuous phase temperature of 25 °C. It had relatively uniform emulsion droplets, a narrow size distribution. The resultant emulsion was solidified by spray drying of aqueous solution containing liquid emulsion and dextran as a hydrophilic solid carrier. The release rate of the drug from the solid emulsion at 15 min was significantly higher than that of itraconazole powder. Furthermore, the

solid emulsion gave significantly higher AUC and C_{max} but shorter T_{max} in rats than did itraconazole powder. Thus, the present study has demonstrated the potential utility of SPG membrane emulsification combined with spray drying technique for development of itraconazole-loaded solid emulsion with increased solubility, release rate and bioavailability.

Acknowledgment

This research was supported by the Basic Science Research Program through National Research Foundation of Korea (NRF) funded by the Ministry of Education, Science and Technology (No. 2010-0024185).

References

Al-Marzouqi, A., Shehatta, I., Jobe, B., Dowaidar, A., 2006. Phase solubility and inclusion complex of itraconazole with beta-cyclodextrin using supercritical carbon dioxide. J. Pharm. Sci. 95, 292–304.

Babak, V.G., Baros, F., Boulanouar, O., Boury, F., Fromm, M., Kildeeva, N.R., Ubrich, N., Maincent, P., 2007. Impact of bulk and surface properties of some biocompatible hydrophobic polymers on the stability of methylene chloride-in-water miniemulsions used to prepare nanoparticles by emulsification–solvent evaporation. Colloids Surf. B 59, 194–207.

Balakrishnan, P., Lee, B., Oh, D., Kim, J., Hong, M., Jee, J., Kim, J., Yoo, B., Woo, J., Yong, C., 2009. Enhanced oral bioavailability of dexibuprofen by a novel solid self-emulsifying drug delivery system (SEDDS). Eur. J. Pharmacol. 72, 539–545.

Chen, H., Shi, S., Zhao, M., Zhang, L., He, H., Tang, X., 2011. A lyophilized etoposide submicron emulsion with a high drug loading for intravenous injection: preparation, evaluation, and pharmacokinetics in rats. Drug Dev. Ind. Pharm. 36, 1444–1453.

Choi, H., Lee, B., Han, J., Lee, M., Park, K., Yong, C., Kim, Y., Kim, C., 2001. Terfenadine-β-cyclodextrin inclusion complex with antihistaminic activity enhancement. Drug Dev. Ind. Pharm. 27, 857–862.

Choi, H., Oh, Y., Kim, C., 1998. In situ gelling and mucoadhesive liquid suppository containing acetaminophen: enhanced bioavailability. Int. J. Pharm. 165, 23–32.

Craig, D.Q.M., Barker, S.A., Banning, D., Booth, S.W., 1995. An investigation into the mechanisms of self-emulsification using particle size analysis and low frequency dielectric spectroscopy. Int. J. Pharm. 114, 103–110.

Ee, S., Duan, X., Liew, J., Nguyen, Q., 2008. Droplet size and stability of nanoemulsions produced by the temperature phase inversion method. Chem. Eng. J. 140, 626–631.

Joscelyne, S., Trägårdh, G., 1999. Food emulsions using membrane emulsification: conditions for producing small droplets. J. Food Eng. 39, 59–64.

Kim, C., Park, J., 2004. Solubility enhancers for oral drug delivery: can chemical structure manipulation be avoided? Am. J. Drug Deliv. 2, 113–130.

Kobayashi, I., Nakajima, M., Mukataka, S., 2003. Preparation characteristics of oil-in-water emulsions using differently charged surfactants in straight-through microchannel emulsification. Colloids Surf. A 229, 33–41.

Li, D., Oh, Y., Lim, S., Kim, J., Yang, H., Sung, J., Yong, C., Choi, H., 2008. Novel gelatin microcapsule with bioavailability enhancement of ibuprofen using spray-drying technique. Int. J. Pharm. 355, 277–284.

Liu, W., Yang, X.L., Ho, W.S., 2011. Preparation of uniform-sized multiple emulsions and micro/nano particulates for drug delivery by membrane emulsification. J. Pharm. Sci. 100, 75–93.

McClements, D., 1999. Food Emulsion: Principles, Practice, and Techniques. CRC Press, Boca Raton, FL.

Myers, S., Shively, M., 1993. Solid-state emulsions: the effects of maltodextrin on microcrystalline aging. Pharm. Res. 10, 1389–1391.

Nakashima, T., Shimizu, M., Kukizaki, M., 1991. Membrane emulsification by microporous glass. Key Eng. Mater. 61–62, 513–516.

Nakashima, T., Shimizu, M., 1993. Preparation of monodispersed O/W emulsion by porous glass membrane. Kagaku Kogaku Ronbun. 19, 984–990.

Nakashima, T., Shimizu, M., Kukizaki, M., 2000. Particle control of emulsion by membrane emulsification and its application. Adv. Drug Deliv. Rev. 45, 47–56.

Nazir, H., Lv, P., Wang, L., Lian, G., Zhu, S., Ma, G.H., 2011. Uniform-sized silicone oil microemulsions: preparation, investigation of stability and deposition on hair surface. J. Colloid Interface Sci. 364, 56–64.

Ni, H.M., Kawaguchi, H., Endo, T., 2007. Preparation of pH-sensitive hydrogel microspheres of poly(acrylamide-co-methacrylic acid) with sharp pH-volume transition. Colloid Polym. Sci. 285, 819–826.

Odds, F., Ors, M., Van Dorsselaer, P., Van Gerve, F., 2000. Activities of an intravenous formulation of itraconazole in experimental disseminated *Aspergillus, Candida, and Cryptococcus* infections. Antimicrob. Agents Chemother. 44, 3180–3181.

Omi, S., Kaneka, A., Nakayama, A., Katami, K., Taguchi, T., Iso, M., Nagai, M., Ma, M.G.-H., 1997. Application of porous microspheres prepared by SPG emulsification as immobilizing carriers of glucamylase (GLuA). J. Appl. Polym. Sci. 65, 2655–2664.

Oh, D.H., Balakrishnan, P., Oh, Y.K., Kim, D.D., Yong, C.S., Choi, H.G., 2011. Effect of process parameters on nanoemulsion droplet size and distribution in SPG membrane emulsification. Int. J. Pharm. 404, 191–197.

Saag, M., Dismukes, W., 1988. Azole antifungal agents: emphasis on new triazole. Antimicrob. Agents Chemother. 32, 1–8.

Schröder, V., Behrend, O., Schubert, H., 1998. Effect of dynamic interfacial tension on the emulsification process using microporous ceramic membrane. J. Colloid Interface Sci. 202, 334–340.

Schröder, V., Schubert, H., 1999. Production of emulsions using microporous, ceramic membranes. Colloids Surf. A: Physicochem. Eng. Aspects 152, 103–109.

Shafiq, S., Shakeel, F., Talegaonkar, S., Ahmad, F.J., Khar, R.K., Ali, M., 2007. Development and bioavailability assessment of ramipril nanoemulsion formulation. Eur. J. Pharm. Biopharm. 66, 227–243.

Shively, M., Thompson, D., 1995. Oral bioavailability of vancomycin solid-state emulsions. Int. J. Pharm. 117, 119–122.

Society of Toxicology (SOT), 2008. Guiding Principles in the Use of Animals in Toxicology., http://www.toxicology.org/AI/FA/guidingprinciples.pdf.

Soheil, J., Hussein, G., Zahra, B., Beheshteh, S., 2008. Electrolyte effect on mixed micelle and interfacial properties of binary mixtures of cationic and nonionic surfactants. J. Colloid Interface Sci. 318, 449–456.

Tadros, T., Izquierdob, P., Esquenab, J., Solans, C., 2004. Formation and stability of nano-emulsions. Adv. Colloid Interface 108, 303–318.

Torrado, S., Lopez, M., Torrado, G., Bolas, F., Cadorniga, R., 1997. A novel formulation of albendazole solution: oral bioavailability and efficacy evaluation. Int. J. Pharm. 156, 181–187.

Tsukada, Y., Hara, K., Bando, Y., Huang, C.C., Kousaka, Y., Kawashima, Y., Morishita, R., Tsujimoto, H., 2009. Particle size control of poly(DL-lactide-co-glycolide) nanospheres for sterile applications. Int. J. Pharm. 370, 196–220.

Vladisavljević, G.T., Schubert, H., 2003. Influence of process parameters on droplet size distribution in SPG membrane emulsification and stability of prepared emulsion droplets. J. Membr. Sci. 225, 15–23.

Vladisavljević, G.T., Williams, R.A., 2005. Recent developments in manufacturing emulsions and particulate products using membranes. Adv. Colloid Interface Sci. 113, 1–20.

Vladisavljević, G.T., Shimizu, M., Nakashima, T., 2006. Production of multiple emulsions for drug delivery systems by repeated SPG membrane homogenization: influence of mean pore size, interfacial tension and continuous phase viscosity. Int. J. Pharm. 273, 171–182.

Vladisavljević, G.T., Lambrich, U., Nakajima, M., Schubert, H., 2007. Production of O/W emulsions using SPG membranes, ceramic α-aluminium oxide membranes, microfluidizer and a silicon microchannel plate—a comparative study. Colloid Surf. A 232, 199–207.

Wei, Q., Li, J., Qian, B., Fang, B., Zhao, C., 2009. Preparation, characterization and application of functional polyethersulfone membranes blended with poly(acrylic acid) gels. J. Membr. Sci. 337, 266–273.

Yasuno, M., Nakajima, M., Iwamoto, S., Maruyama, T., Sugiura, S., Kobayashi, I., Shono, A., Satoh, K., 2002. Visualization and characterization of SPG membrane emulsification. J. Membr. Sci. 210, 29–37.

Yong, C.S., Li, D.X., Oh, D.H., Kim, J.A., Yoo, B.K., Woo, J.S., Rhee, J.D., Choi, H.G., 2005. Retarded dissolution of ibuprofen in gelatin microcapsule by cross-linking with glutaraldehyde. Arch. Pharm. Res. 29, 431–534.

Yan, Y., Kim, J., Kwak, M., Yoo, B., Yong, C., Choi, H., 2011. Enhanced oral bioavailability of curcumin via a solid lipid-based self-emulsifying drug delivery system using a spray-drying technique. Biol. Pharm. Bull. 34, 1179–1186.